Published in final edited form as:
APMIS. 2008 ; 116(7-8): 695–715. doi:10.1111/j.1600-0463.2008.01148.x.

Imaging angiogenesis and the microenvironment

DAI FUKUMURA and **RAKESH K. JAIN**
Edwin L. Steele Laboratory, Department of Radiation Oncology, Massachusetts General Hospital and Harvard Medical School, Boston, MA, USA

Abstract

Intravital microscopy has provided unprecedented insights into tumor pathophysiology, including angiogenesis and the microenvironment. Tumor vasculature shows an abnormal organization, structure, and function. Tumor vessels are leaky, blood flow is heterogeneous and often compromised. Vascular hyperpermeability and the lack of functional lymphatic vessels inside tumors causes elevation of interstitial fluid pressure in solid tumors. These abnormalities form physiological barriers to the delivery of therapeutic agents to tumors and also lead to a hostile microenvironment characterized by hypoxia and acidosis, which hinders the effectiveness of anti-tumor treatments such as radiation therapy and chemotherapy. In addition, host-tumor interactions regulate expression of pro- and anti-angiogenic factors, resulting in pathophysiological characteristics of the tumor. On the other hand, in a physiological setting, angiogenic vessels become mature and form long-lasting functional units. Restoring the balance of pro- and anti-angiogenic factors in tumors may “normalize” tumor vasculature and thus improve its function. Administration of cytotoxic therapy during the vascular normalization would enhance its efficacy.

Keywords

Intravital microscopy; angiogenesis; lymphangiogenesis; tumor; stromal cells; micro-environment; tumor dormancy

Angiogenesis is one of the critical steps required for solid tumors to grow beyond their dormant state (1). The resulting tumor vasculature is not a simple supply line of nutrients to tumors. It governs pathophysiology of solid tumors and thus tumor growth, invasion, metastasis and response to various therapies. Intravital microscopy has provided unprecedented molecular, cellular, anatomical and functional insights into tumor pathophysiology, including angiogenesis and the microenvironment (2). In this review, we discuss the structure and function of tumor vasculature, the resulting abnormal microenvironment, causes and consequences of these abnormalities, physiological angiogenesis and potential normalization of the tumor vasculature and microenvironment, aspects which are associated with an escape from tumor dormancy.

INTRAVITAL MICROSCOPY

To study tumor angiogenesis, vasculature and microenvironment *in vivo*, invasive or non-invasive approaches can be used. Histological and molecular techniques allow subcellular and molecular level analyses. However, these invasive techniques are not suitable for kinetic and/or functional studies. Non- or minimally invasive imaging techniques can obtain

Dai Fukumura or Rakesh K. Jain, Edwin L. Steele Laboratory for Tumor Biology, Department of Radiation Oncology, Massachusetts General Hospital and Harvard Medical School, 100 Blossom Street – Cox 7, Boston, MA 02114, USA. dai@steele.mgh.harvard.edu or jain@steele.mgh.harvard.edu.

temporal dynamics and quantitatively determine physiological functions. However, clinically available imaging techniques such as PET, CT, and MRI do not have sufficient spatial resolution to visualize cellular and subcellular levels (3). Intravital microscopy (IVM), an optical microscopy technique applying to study living organisms, can overcome these limitations. IVM has the highest spatial resolution among imaging techniques applicable for living tissues (1–10 μm) and provides insights into various molecular and cellular processes *in vivo* (2).

To perform quantitative IVM, four essential components are required: (i) a tissue preparation that permits optical access, (ii) a molecular probe that can be detected by a microscope, (iii) a microscope and detection system, and (iv) computer algorithms and mathematical models that can extract parameters of interest from the imaging data set (Fig. 1A).

The following three different kinds of tissue preparations can be used for IVM: (i) *in situ* preparations; (ii) acute (exteriorized) tissue preparations; and (iii) chronic-transparent windows. Each preparation has advantages and disadvantages. *In situ* preparation such as ear and tail does not require any invasive preparation, but accessible tissues are limited. Acute exteriorization can be applied to virtually any tissue with variable degrees of difficulty. However, the duration and frequency of the observation is limited and the preparation procedures may affect the physiological parameters. Window models such as dorsal skinfold chamber and cranial window require surgical implantation and sufficient recovery time after the implantation, but permit chronic and repeated observations thereafter.

Once the tissue preparation is ready for observation, the animal is transferred to the specially designed microscope stage and the tissue is visualized using an appropriate exogenous or endogenous molecular probe depending on the parameters of interest (Table 1).

Historically, the superior resolution of light microscopy has come at the expense of diminished depth penetration (2). Light scattering and absorption within tissues limit typical epifluorescence and confocal laser scanning microscopes (CLSM) to penetrating ~100 microns into the body. The multiphoton laser-scanning microscope (MPLSM) has recently emerged as a useful technique for high-resolution, non-destructive, chronic imaging within living tissues (4). MPLSM has markedly superior depth penetration in tissues and in combination with chronic window models allows repetitive imaging at depths of several hundred microns within living tissue while retaining submicron spatial resolution (4).

IMAGING TUMOR VESSELS

Abnormal blood vessel architecture and function in tumors

The most common application of IVM is to determine the size and architecture of tumors and their vasculature, parameters often of interest with regard to dormant tumors and metastases. To visualize blood vessels, RBCs can be used as an endogenous contrast agent under conventional transillumination, linearly polarized light (5), or optical coherence tomography (6). For fluorescence microscopy, high-molecular-weight fluorescent tracers (e.g. FITC-conjugated 2000 kDa dextran) are injected to demarcate the blood vessel before it begins to leak appreciably into the extravascular compartment. Vessel diameter, length, surface area and volume as well as branching patterns and intercapillary distance in a growing or regressing tumor have been described (7,8). The normal microvessels consist of differentiated units such as arterioles, capillaries and venules, and form a well-organized architecture with dichotomous branching and hierarchic order (Fig. 1B) (9). In contrast, tumor vessels are dilated, saccular, tortuous, and heterogeneous in their spatial distribution

(Fig. 1C) (10). Tumor vasculature is disorganized and has trifurcations and branches with uneven diameters. Fractal analysis of normal and tumor vascular networks reveals that the former are optimally designed to provide nutrients by diffusion to all normal cells (so-called diffusion-limited aggregation), whereas the latter are restricted by the mechanical properties of the matrix (called invasion percolation) (11,12). The molecular mechanisms causing these abnormal vascular architectures are not well understood, but the imbalance of pro- and anti-angiogenic factors is considered to be a key contributor (13). Solid (mechanical) stress generated by proliferating tumor cells also compresses vessels in tumors (14,15). The combination of both molecular and mechanical factors may render the tumor vasculature abnormal.

Furthermore, blood perfusion in tumors is spatially and temporally heterogeneous (4,7,10,16–19). Overall perfusion rates (blood flow rate per unit volume) in many tumors are lower than those in many normal tissues and the average RBC velocity in tumor vessels can be an order of magnitude lower than in normal vessels (Fig. 1D, E) (4,7,16). Unlike normal vessels, RBC velocity is independent of the diameter of tumor vessels. Arteriovenous pressure difference and flow resistance govern blood flow in a vascular network. Flow resistance is a function of geometric (vascular architecture) and viscous (blood viscosity, rheology) resistances. Abnormalities in both vasculature and viscosity increase the resistance to blood flow in tumors (10). Focal leaks, which often exist in some of the tumor vessels, may also compromise the downstream blood flow. The heterogeneity of tumor blood flow hinders the delivery of therapeutic agents to tumors and causes an abnormal microenvironment in tumors. The latter, in turn, compromises the effectiveness of various therapies, and selects for more aggressive and metastatic cancer cells (20).

IVM observations also reveal that leukocyte-endothelial interactions are generally low and heterogeneous in tumor vessels (17–19,21–24). Exogenously injected activated lymphocytes can adhere to some tumor vessels but not others (25,26). These heterogeneous leukocyte adhesions may reflect heterogeneous expression of adhesion molecules on tumor vessels. Local imbalance of angiogenic factor signaling may also contribute to these heterogeneities. VEGF up-regulates various adhesion molecules, including ICAM-1, VCAM-1, and E-selectin, whereas bFGF and Ang-1 downregulate these adhesion molecules in vascular endothelial cells (27–29). The link between angiogenesis (VEGF) and inflammation (leukocyte adhesion) has also been shown in a number of *in vivo* models (30–32). Furthermore, myeloid cells migrated in tumors facilitate angiogenesis and tumor growth, and in some cases mediate resistance to anti-angiogenic treatments (33,34).

Vessel wall structure is abnormal in tumors (35–37). Large interendothelial junctions, increased numbers of fenestrations, vesicles and vesicovacuolar channels, and a lack of normal basement membrane are often found in tumor vessels (38,39). Perivascular cells have abnormal morphology and heterogeneous association with tumor vessels. In agreement with these structural alterations in the tumor vessel wall, vascular permeability of solid tumor vessels is generally higher than that of most normal vessels (40–42). Extravasation of molecules from the bloodstream occurs by diffusion, convection, and, to some extent, by transcytosis in an exchange vessel. Diffusion is considered to be the major form of transvascular transport in tumors (43). The diffusive permeability of a molecule depends on its size, shape, charge, and flexibility as well as the transvascular transport pathway.

Owing to the physical limitations of optical microscopy, it is not possible to directly measure the dimensions of submicron structures *in vivo*. However, such measurements can be made by monitoring the movement of fluorescent nanoparticles in the tissue. By titrating the extravasation of nanoparticles of increasing size, we found that the cut-off size of “pores” in the walls of tumor vessels varied from ~100 nm to 2 μm depending on the tumor

type, the location of its growth, and whether it is growing or regressing (42,44). The large pore size characteristic of most tumor vessels means that they lack permselectivity (45). Furthermore, the biggest challenge in transvascular transport in tumors stems from the spatial and temporal heterogeneity in permeability (44,45), which restricts access to some regions of tumors. However, it is possible to lower the vascular permeability of a tumor by blocking VEGF signaling (8,46). Anti-angiogenic therapy can alleviate vascular hyperpermeability-associated abnormalities such as high interstitial fluid pressure and edema, and thus improve patient symptoms and treatment outcome (47,48).

Abnormal lymphatics in tumors

IVM has also provided powerful insights into the pathophysiology of lymphatics in and around tumors. In most normal tissues, excess fluid and macromolecules are reabsorbed by the lymphatic capillaries and brought back to the thoracic duct. Using two different intravital methods, fluid velocity in the lymphatic capillaries was ~1 to 10 μm/s—considerably faster than the interstitial fluid velocity (~ 0.1 μm/s), but slower than blood velocity (~ 100–1000 μm/s) (49–51). Fluorescence microlymphangiography of tumors growing in the tail of mice has shown that the lymphatics in the tumor margin are hyperplastic, similar to those in the skin of mice engineered to overexpress VEGF-C, a lymphangiogenic growth factor, in their keratinocytes (52–54). The diameters of these lymphatics in the tumor margin increase even further in tumors that overexpress VEGF-C (53,55). Surprisingly, overexpression of VEGF-C does not induce any functional lymphatics within these tumors. Proliferating tumor cells in a confined space create mechanical stress (solid stress) which compresses intratumor lymphatic vessels (14). Consequently, there are no functional lymphatic vessels inside solid tumors (52,53). Even if the structures with lymphatic endothelial markers are present in tumors, they do not transport fluid or macromolecules. The lack of functional lymphatics within tumors is a key contributor to the interstitial hypertension measured in animal and human tumors (56,57). In contrast to the lack of functional intratumor lymphatics, functional lymphatic vessels are present in the tumor margin and the peritumoral tissue (Fig. 1F, G) (53,58). These peritumoral lymphatic vessels are hyperplastic and collect fluid, growth factors and cells exiting from tumors. IVM can detect GFP-labeled tumor cells traveling in these peritumor lymphatics and their arrival in the nearby lymph node, indicating that the hyperplastic lymphatics in the tumor margin carry metastatic tumor cells and mediate metastases via the lymphatic system.

IMAGING MICROENVIRONMENT

Abnormal metabolic environment in tumors

Molecular probes that change their optical properties as a function of pO_2 and pH have been successfully used to monitor the metabolic microenvironment in tumors by intravital microscopy (59). Hypoxia and acidosis are the hallmarks of an abnormal metabolic environment in solid tumors (Fig. 2A) (59–61). Owing to their abnormal structure and function, tumor vessels are unable to deliver adequate levels of nutrients and oxygen to tumors and to remove acidic waste products out of tumors. Local imbalance of angiogenesis and tumor cell proliferation makes hypovascular regions in tumors. The regions far from blood vessels become chronically hypoxic (chronic or diffusion-limited hypoxia) and acidic (Fig. 2A). As discussed, blood flow in tumor vessels is temporally heterogeneous. The intermittent blood flow causes periodical hypoxia in a tumor which is called acute or perfusion-limited hypoxia (62,63). Even the presence of blood flow does not guarantee the delivery of oxygen in solid tumors. High-resolution intravital microscopy revealed that some of the perfused tumor vessels carry almost no oxygen and there is no clear relationship between blood flow rate and oxygen tension (pO_2) of individual tumor vessels (59). Moreover, simultaneous high-resolution mapping of tissue pO_2 and (phosphorescence

quenching microscopy) and pH (fluorescence ratio-imaging microscopy) revealed that there is a lack of spatial correlation among these parameters (59). These findings have significant implications since both pO_2 and pH are important determinants of tumor growth, metabolism, and response to a variety of therapies (64,65).

Radiation therapy and many chemotherapeutics generate free radicals in the presence of oxygen and damage DNA (64,65). Thus, hypoxia in solid tumors significantly reduces sensitivity to treatments with radiation and these drugs. Since intracellular pH is neutral, acidic extracellular pH decreases the cellular uptake of weakly base drugs, and thus their efficacy (64). Hypoxia and/or acidosis also compromise the function of immune cells targeting tumors and reduce the efficacy of host immune response and cell-based therapies. The hostile metabolic environment in tumors may select for tumor cells that are more malignant, aggressive and genetically unstable, and less susceptible to apoptosis, thus rendering them resistant to various therapies and highly invasive and metastatic (66–68). Finally, both hypoxia and acidic pH can induce expression of angiogenic factors, and thus contribute to growth and metastasis of tumors (69).

Regulation of angiogenic gene expression by metabolic microenvironment

The most exciting and innovative application of molecular imaging would be the monitoring of gene expression and regulation *in vivo*. The recent discovery and commercial availability of live fluorescent reporters such as blue, cyan, green, yellow, red and far red fluorescent proteins (BFP. CFP, GFP, YFP, DsRed and HcRed) has made this feasible. By creating transgenic cell lines or animals that harbor GFP or its spectral variants under the control of the promoter of the gene of interest, it is now possible to monitor promoter activity as well as the microenvironmental parameters that regulate this activity (70,71).

Hypoxia upregulates various angiogenic growth factors, including vascular endothelial growth factor (VEGF), angiopoietin (Ang) 2, platelet-derived growth factor (PDGF), placenta growth factor (PlGF), transforming growth factor α (TGFα), interleukin (IL)-8, and hepatocyte growth factor (HGF) (60). Of the various molecules involved in sensing and responding to hypoxia, hypoxia-inducible factor 1α (HIF1α) is considered to be the master regulator of oxygen homeostasis (72). This transcriptional factor is upregulated in a number of human tumors (60). HIF1α binds to the hypoxia-responsive element (HRE) in the promoter of hypoxia-responsive genes such as VEGF, PDGF and TGFα and induces their expression (60,72). A few other factors, such as IL-8 and PlGF, are activated by HIF-independent mechanisms (60,73). Hypoxia may also play an important role in the angiogenic switch that is required for tumor growth and expansion in mass.

Low extracellular pH causes stress-induced alteration of gene expression, including the up-regulation of VEGF and IL-8 in tumor cells *in vitro* (74). Despite its importance, the effect of the low and heterogeneous interstitial pH on VEGF expression *in vivo*, especially in relationship to hypoxia, remained unknown for many years due to the lack of appropriate techniques and animal models. The combination of fluorescence ratio imaging microscopy for pH measurements (75), phosphorescence quenching microscopy for pO_2 measurements (76) and transgenic technology for visualization of VEGF promoter activity (70) has allowed the coordinated study of pH, pO_2, and VEGF expression *in vivo* (Fig. 2B) (71). Detailed analysis indicated that in low pH or oxygenated regions, tissue pH, but not pO_2, regulates VEGF promoter activity. Conversely, in hypoxic or neutral pH regions, tissue pO_2, and not pH, regulates VEGF expression (71). Tissue pO_2 and pH appeared to regulate VEGF transcription in tumors independently. In fact, analysis of the VEGF promoter region revealed that acidic pH induces VEGF expression via the Ras-ERK1/2-AP1 pathway but not the HIF-HRE-mediated pathway (74). Taken together these data suggest that two key

microenvironmental parameters in solid tumors regulate angiogenic factors in a complementary manner.

Involvement of host stromal cells in tumor angiogenesis

It is becoming increasingly apparent that the development and pathophysiology of a tumor cannot be explained simply by the genes in the tumor cells (77). We are beginning to understand that host stromal cells profoundly influence many steps of tumor progression, such as tumor cell proliferation, invasion, angiogenesis, metastasis, and even malignant transformation (70,78–83). Interactions between the diverse cell types within a tumor, via both soluble factors and direct cell-to-cell contact, play an important role in the induction, selection, and expansion of the neoplastic cells. Successful tumor cells are those that have acquired the ability to co-opt their normal neighbors by inducing them to release abundant fluxes of growth-stimulating signals (77,79,81).

Intravital observation of tumors grown in a GFP reporter mouse revealed that stromal fibroblasts express VEGF in tumors especially abundantly at the host-tumor interface (70) (Fig. 2C). Furthermore, VEGF-expressing stromal cells co-localize with the vasculature and even surround tumor blood vessels deep inside the tumor (4) (Fig. 2C). These findings suggest that activated fibroblasts are involved in angiogenesis, fortification of blood vessels, and function of these vessels. In fact, co-implantation of fibroblasts enhanced the tumorigenicity of breast cancer cells *in vivo* (84). Carcinoma-associated fibroblasts promote tumor growth and angiogenesis through secretion of SDF-1/CXCL12 (85). Furthermore, mesenchymal stem cells increase breast cancer metastasis via secretion of CCL5/RANTES (86). In addition to fibroblasts, inflammatory cells recruited to tumors may also promote (rather than eliminate) angiogenesis and tumor cell growth (80,87). Some studies show the relative contribution of stromal cells and tumor cells in the expression of VEGF in tumors. For example, teratomas derived from VEGF-deficient embryonic stem cells (ES cells) show VEGF levels and angiogenic activity about one-half of that in tumors derived from wild-type ES cells, suggesting that host stromal cells can produce approximately half of the total VEGF in this tumor type (32). On the other hand, late-stage orthotopic pancreatic tumors expressed significantly higher tumor cell-derived VEGF compared to early-stage or ectopically grown tumors (88). The ratio of tumor-to-host-derived VEGF and other growth factors may vary depending on tumor type, stage, and organ site.

Regulation of angiogenesis and vessel functions by organ microenvironment

Angiogenesis and functions of resultant vessels differ significantly between the same tumors grown in different host organs (2,89). For example, murine melanomas grown in a cranial window have higher vessel density and branching, and relatively smaller vessel size as compared to those in the same tumors grown in a dorsal skin chamber (Fig. 2D) (90). A human glioma (HGL21) has fairly leaky vessels when grown subcutaneously in immunodeficient mice, but it exhibits blood-brain barrier properties in the cranial window (91). Furthermore, the vascular pore cut-off size (the maximum functional pore size for transvascular transport of macromolecules through the vessel wall) in various tumors decreased when the tumors were grown in the cranial window as compared to the dorsal skin chamber (42). Organ-specific upregulation of angiogenic factors is one of the mechanisms causing differential angiogenic activity. In agreement with the higher angiogenic activity (Fig. 2D), the murine melanomas exhibit higher tissue nitric oxide levels when grown in the cranium compared to the same tumors grown subcutaneously (90). Human renal cell carcinoma xenografts grown orthotopically in the kidneys of immunodeficient mice were highly vascularized and metastatic, and expressed 10- to 20-fold higher levels of bFGF mRNA than those from the same tumor grown subcutaneously (92). Human colon cancer and melanoma grown in the liver expressed lower levels of VEGF and IL-8 mRNA,

respectively, and had a lower vessel density than those in subcutaneous tissue (19,93). The expression of endogenous anti-angiogenic factors is also regulated by the organ-specific host-tumor interaction. Human gall bladder primary tumors inhibit angiogenesis and growth of secondary tumors at a distant site in a TGFβ1-dependent mechanism. This result was observed when the primary tumors were grown in the gall bladder (orthotopic) but not in the subcutaneous space (ectopic) (94).

Furthermore, the response of the blood vessels to a given stimuli may also vary depending on the host organ site and host-tumor interaction. With the presence of a blood-brain barrier, a significantly higher amount of VEGF was required to induce vascular hyperpermeability in normal vessels in the cranial window than in the dorsal skin chamber (44). On the other hand, the cranial environment is more angiogenic and forms new vessels faster than the subcutaneous tissue in response to a given angiogenic factor such as VEGF and bFGF (95). These differences are presumably due to differences in the phenotype of vascular endothelial cells, which is defined by their origin, by cell-cell and cell-matrix interactions, and by the local microenvironment. These findings indicate that VEGF level alone may not be a sufficient predictor of angiogenesis or vascular permeability in the tumors growing in different organs. Indeed, the vascular permeability of LS174T human colon cancer grown in the liver versus subcutaneous space was inversely correlated with the expression levels of VEGF at these sites, while angiogenesis paralleled the VEGF levels (19). Conversely, higher VEGF expression and permeability but lower angiogenesis was observed in ZR75 human breast cancers grown in the mammary fat pad (primary site) compared to those grown in the cranial window (meta-static site) (96). Knowledge of organ-dependent profiles of gene expression and protein level as well as responsiveness to these factors, in stromal cells and tumor cells from different organ microenvironments, will provide new insights into tumor biology and should allow us to understand why a given tumor behaves differently in different organs.

IMAGING PHYSIOLOGICAL ANGIOGNESIS

Adipogenesis and angiogenesis

Fat tissue is highly vascularized (Fig. 3A) and has long been known to be highly angiogenic. Surgeons have been using adipose tissue grafts to promote wound healing and to revascularize ischemic tissues since the early 17th century. Adipocytes produce a variety of angiogenic factors, including VEGF, basic fibroblast growth factor (bFGF), leptin and matrix metalloproteinases (MMPs) (97). Obese patients exhibit elevated serum VEGF level (98). Several recent studies demonstrated that fat tissue development is angiogenesis dependent by using anti-angiogenic/anti-vascular agents as well as genetically engineered animal models (99–102).

Furthermore, we have shown that there is reciprocal regulation between adipogenesis (fat cell differentiation) and angiogenesis, and that VEGF signaling mediates this relationship. Preadipocytes differentiate into fat-storing mature adipocytes after implantation in the mouse dorsal skin chamber model. This process is accompanied by a vigorous angiogenic response. When adipogenesis in the preadipocytes is genetically inhibited, there is no angiogenesis. On the other hand, when angiogenesis is inhibited by an anti-VEGF receptor antibody, the proliferation and differentiation of preadipocytes is also inhibited (Fig. 3A). This paracrine reciprocal regulation between endothelial cells (growth of new blood vessels) and preadipocytes (differentiation into adipocytes) is mediated at least in part by a VEGF-induced factor that promotes adipogenesis (101).

It should be noted that newly developed blood vessels induced by implanted preadipocytes become mature and stable with the maturation of adipose tissues. Initially vessel structure is

mesh like, similar to tumor vessels. However, these vessels were remodeled and differentiated into functional units such as arterioles, capillaries and venules (Fig. 3A). As many angiogenesis models develop only immature blood vessels, an adipogenesis model provides an ideal platform to study the complete process of angiogenesis, vessel remodeling and maturation in adult tissues.

Tissue engineered blood vessels

The formation of new blood vessels in adult tissues was thought to occur exclusively through the process of angiogenesis, where the newly formed vessels are derived from preexisting blood vessels (103,104). The alternate process, vasculogenesis, defined as the *de novo* formation of blood vessel from endothelial progenitor cells, was thought to occur only during development (105). The discovery of circulating endothelial and smooth muscle progenitor cells along with the subsequent *in vivo* studies of their functions caused a paradigm shift (106,107).

Although endothelial precursor cells can initiate the process of neovascularization, they cannot complete this process by themselves. Endothelial cells initially form a naked tube that is highly permeable and unstable (108). For vessel maturation and stabilization, the naked endothelial tube undergoes a series of steps to recruit and to differentiate perivascular cells to line the outer layer of the vessels (109,110). Perivascular cells such as vascular smooth muscle cells and pericytes are thought to provide the vessels with structural integrity, lay down basement membrane, and provide the endothelial cells with necessary survival factors (111).

To date the emphasis in therapeutic angiogenesis has been almost exclusively on studies of endothelial cells. Engineered blood vessels have often been found to be immature and unstable (112), and the lack of proper perivascular cell support is likely to be one of the main reasons for this instability. We have shown that engineered vessels can become long lasting with stable vasculature by incorporating perivascular cells (113) (Fig. 3B). Co-implantation of human umbilical vein endothelial cells (HUVECs) and 10T1/2 cells, a mesenchymal precursor cell line that is capable of differentiating into perivascular cells through heterotypic interaction with endothelial cells (109), results in small diameter blood vessels that remain patent for over 1 year with good functionality, and display proper coverage of perivascular cells. While these results are encouraging, this model is not immediately applicable in the clinic because HUVECs and 10T1/2 cells are not immunocompatible with human patients.

Human embryonic stem cells (hESCs) are pluripotent, capable of differentiating into all cell types in a body. We and others have demonstrated that hESC-derived endothelial cells have the ability to form functional blood vessels *in vivo* (114,115). We observed that some of the hESC-derived blood vessels persisted for more than 150 days as functional, blood-perfused vessels. However, there are significant scientific and ethical challenges when using hESCs in the clinic. Recently we and others have been able to reproduce these results using human bone marrow-derived mesenchymal stem cells (hMSCs) or human saphenous vein smooth muscle cells (HSVSMCs) instead of the 10T1/2 cell line, and using endothelial progenitor cells from umbilical cord blood instead of HUVECs (116–118). By using cell sources that are compatible with the human body, these studies have brought our method one step closer to possible clinical utilization.

IMAGING THERAPEUTIC RESPONSE: NORMALIZATION OF TUMOR VASCULATURE AND MICROENVIRONMENT

Tumor response to a new treatment is typically assessed by the reduction or stabilization of tumor size and survival time of the animals. Various parameters obtained by IVM can provide mechanistic and integrated insights into the response of tumors. These insights have led to new strategies for improving cancer detection and treatment. For an example, during the course of various direct and indirect anti-angiogenic therapies, tumor vessels occasionally develop a normal-like phenotype: their diameter decreases, they become straighter and less tortuous, and their fractal dimension begins to decrease toward the diffusion-limited aggregation regime (8,12,31,46,119). As discussed earlier, excess production of proangiogenic molecules and/or diminished production of anti-angiogenic molecules may cause the abnormalities in vessels and microenvironment in tumors resulting in insufficient drug delivery and therapeutic efficacy (13). Targeting angiogenic signaling may reverse these abnormalities and improve concomitantly administered cytotoxic therapies. Indeed, anti-VEGF treatments have been shown to improve tumor vasculature and micro-environment in various tumor models (8,39,120–123). Bevacizumab (anti-VEGF antibody) and DC101 (anti-VEGFR2 antibody) prune some tumor vessels and remodel the remaining vasculature in human colon cancer and glioma xenografts as well as murine breast cancers so that it more closely resembles the normal vasculature (Fig. 4A) (8,39,120). The anti-VEGF treatments reduce the size and length as well as permeability of these abnormally dilated and tortuous vessels (8,39,120). The “normalized” vasculature during the anti-VEGFR2 treatment has greater coverage of perivascular cells and a more normal thickness of basement membrane in breast cancers, squamous cell carcinomas and gliomas (39,120,124). These changes in tumor vasculature are accompanied by normalization of the tumor microenvironment. Bevacizumab, DC101 and SU11657 (small molecule inhibitor of VEGFRs and PDGFR) decrease tumor IFP in breast, colon cancers and gliomas (120–122). Decreased IFP restores pressure gradient across the blood vessel wall as well as the tumor interstitium, and thus increases drug penetration in tumors (55,120,123). Both Bevacizumab and DC101 improve tumor tissue oxygenation in human glioma xenografts (39,121). As a result, the efficacy of radiation treatments is significantly improved when combined with anti-VEGF treatments (39,121,125).

Similar normalization has been observed following indirect anti-angiogenic treatments, which target upstream signaling of angiogenic factors or modulate response to angiogenic factors. The blockade of human epidermal growth factor receptor (HER)-2 signaling by a neutralizing antibody trastuzumab downregulates angiogenic factors such as VEGF, TGFα, Ang1, and PAI-1, and also induces anti-angiogenic factor thrombospondin-1; thus, trastuzumab acts as an anti-angiogenic cocktail against HER2-expressing tumors (119). Trastuzumab normalizes the vasculature of HER2 over-expressing human breast cancer xenografts (119). Vessels in the trastuzumab-treated tumors have diameters and vascular permeability closer to those of normal vessels (Fig. 4B) (119).

Manipulating levels of nitric oxide (NO), a gaseous mediator involved in many biological processes, including angiogenesis and vessel maturation (126), is an alternative strategy to normalize the disorganized network of blood vessels supplying tumors (127). Many NO functions depend on dose and localization of NO. Vascular endothelial cell-derived NO mediates not only angiogenesis but also perivascular cell recruitment and subsequent stabilization of blood vessels (90). On the other hand, non-vascular NO such as that produced by tumor cells may interfere with vessel maturation in solid tumors. We have shown that eliminating NO production from tumor cells via neuronal NO synthase (nNOS) silencing establishes perivascular NO gradients in human glioma xenografts in mice and normalizes the tumor vasculature (Fig. 4C) (127). Vessels in the nNOS-silenced tumors

were more evenly distributed and less distorted, more associated with perivascular cells and less leaky than those in the control tumors (127). These vascular alterations resulted in improved tumor oxygenation and response to radiation treatment (127). Thus, creation of perivascular NO gradients may be an effective strategy for normalizing abnormal vasculature. Combining the use of angiogenesis inhibitors, which normalize vasculature through a different mechanism, with the blockade of nonvascular NO production may produce even greater improvement in therapeutic outcomes.

FUTURE PERSPECTIVES

Intravital microscopy has provided useful insights into angiogenesis and tumor biology (1,20,128,129). Although there are still limitations, several key challenges are beginning to be resolved with the progress in optical technologies, probes and animal models. Currently, the most widely used microscopy techniques are surface weighted. We would need to study functional parameters inside tumors due to their spatially heterogeneous nature. The advent of multi-photon microscopy (MPLSM) was a major breakthrough since it can provide images over 500 micrometers in depth, depending on the tissue and tracer used (4,130–132). Although it is not sufficient to penetrate entire organs, it can now provide 3-D information *in vivo*. Other optical methods such as optical coherence tomography (OCT) can image further deeper regions (133,134). Although OCT cannot image fluorescent probes as MPLSM does, it can provide complementary structural and functional information. With more research in this area, we may be able to obtain dynamic images of the whole tumor with high spatial resolution in the near future.

Image acquisition rate and speed of imaging are also improving (135–137). High-speed imaging is necessary to capture dynamic events such as blood flow, leukocyte–endothelial interactions, tumor-cell–blood-vessel interactions, and movement of small molecules (138). Furthermore, it will enable high-throughput screening of large 3-D volume of tumors to detect specific cellular interactions, such as incorporation of labeled specific cell populations and the initial stage of colonization of a secondary site/organ by metastatic cancer cells. Such kinetic information is vital for understanding the biology of tumors and for optimizing therapeutic approaches.

Currently, most IVM set-ups are bulky bench top devices. The size and bulk of current devices limits their application. However, an increasing effort is being made to miniaturize the cameras and microscopes to make the whole unit hand-held (139,140). The development of miniaturized endoscopic devices will also allow optical imaging of many interior surfaces of the animal without surgical intervention, and will allow imaging of many other organs and tissues via minimally invasive acute laparoscopy. The prototypes of these microscopes successfully obtained some anatomical and molecular imaging, including blood vessel and nerve morphology, calcium transients, reporter gene expression in brain, skin, bladder, liver and colon, which are optically accessible with minimum invasion (141–144). In the future, such miniaturized microscopes and/or microendoscopes will become commonplace and the regions of patients and experimental animals accessible to optical microscopy will greatly increase.

Molecular probes to interrogate various molecular and cellular processes taking place *in vivo* are also rapidly developing (145,146). Novel nanocrystal probes in combination with live reporters such as GFP and their variants will allow us to image multiple events (visualized by distinct colors and their combination) simultaneously (147). With these improvements in microscopy and probes, *in vivo* microscopy will continue to offer new opportunities for unexpected discoveries in tumor biology as well as cancer detection and treatment.

Acknowledgments

This review is based on the following previous review articles: Jain RK, Munn LL, Fukumura D (2002): Dissecting tumour pathophysiology using intravital microscopy. Nature Reviews Cancer 2:266–76; Jain RK (2005): Normalization of tumor vasculature: An emerging concept in anti-angiogenic therapy. Science 307:58–62; Fukumura D (2005): Role of microenvironment on gene expression, angiogenesis and microvascular functions in tumors. In: Meadows GG, editors. Integration/Interaction of Oncologic Growth. Dordrecht: Springer Science +Business Media B.V., 23–36; Fukumura D & Jain RK (2007): Tumor microenvironment abnormalities: Causes, consequences, and strategies to normalize. Journal of Cellular Biochemistry 101: 937–949; Fukumura D & Jain RK (2007): Tumor microvasculature and microenvironment: Targets for anti-angiogenesis and normalization. Microvascular Research 74:72–84; Jain RK, Booth MF, Padera TP, Munn LL, Fukumura D, Brown E (2008): Applications of Non-Linear Intravital Microscopy in Tumor Biology. In: So P, Masters B, editors. Handbook of Biological Nonlinear Optical Microscopy. Oxford University Press, Oxford, UK, Chapter 29, pp. 735–56. The work summarized here has received continuous support from the National Cancer Institute since 1980, including P01-CA-80124 (R.K. Jain and D. Fukumura), R01-CA85140 (R.K. Jain), R01-CA96915 (D. Fukumura), R01-CA115767–01 (R.K. Jain), and U01-CA084301 (R.K. Jain).

References

1. Folkman, J. Tumor angiogenesis. In: Holland, JF.; Frei, E., III; Bast, RC., Jr, et al., editors. Cancer Medicine. 5. Ontario, Canada: B. C. Decker Inc; 2000. p. 132-52.
2. Jain RK, Munn LL, Fukumura D. Dissecting tumor pathophysiology using intravital microscopy. Nat Rev Cancer 2002;2:266–76. [PubMed: 12001988]
3. Weissleder R. Scaling down imaging: molecular mapping of cancer in mice. Nat Rev Cancer 2002;2:11–8. [PubMed: 11902581]
4. Brown EB, Campbell RB, Tsuzuki Y, Xu L, Carmeliet P, Fukumura D, et al. In vivo measurement of gene expression, angiogenesis, and physiological function in tumors using multiphoton laser scanning microscopy. Nat Med 2001;7:864–8. [PubMed: 11433354]
5. Groner W, Winkelman JW, Harris AG, Ince C, Bouma GJ, Messmer K, et al. Orthogonal polarization spectral imaging: a new method for study of the microcirculation. Nat Med 1999;5:1209–13. [PubMed: 10502828]
6. Thomas MW, Grichnik JM, Izatt JA. Three-dimensional images and vessel rendering using optical coherence tomography. Arch Dermatol 2007;143:1468–9. [PubMed: 18025387]
7. Yuan F, Salehi HA, Boucher Y, Vasthare US, Tuma RF, Jain RK. Vascular permeability and microcirculation of gliomas and mammary carcinomas transplanted in rat and mouse cranial window. Cancer Res 1994;54:4564–8. [PubMed: 8062241]
8. Yuan F, Chen Y, Dellian M, Safabakhsh N, Ferrara N, Jain RK. Time-dependent vascular regression and permeability changes in established human tumor xenografts induced by an anti-vascular endothelial growth factor/vascular permeability factor antibody. Proc Natl Acad Sci USA 1996;93:14765–70. [PubMed: 8962129]
9. Jain RK. Molecular regulation of vessel maturation. Nat Med 2003;9:685–93. [PubMed: 12778167]
10. Jain RK. Determinants of tumor blood flow: a review. Cancer Res 1988;48:2641–58. [PubMed: 3282647]
11. Gazit Y, Berk DA, Leunig M, Baxter LT, Jain RK. Scale-invariant behavior and vascular network formation in normal and tumor tissue. Phys Rev Lett 1995;75:2428–31. [PubMed: 10059301]
12. Baish JW, Jain RK. Fractals and cancer. Cancer Res 2000;60:3683–8. [PubMed: 10919633]
13. Jain RK. Normalization of tumor vasculature: an emerging concept in antiangiogenic therapy. Science 2005;307:58–62. [PubMed: 15637262]
14. Padera TP, Stoll BR, Tooredman JB, Capen D, di Tomaso E, Jain RK. Pathology: cancer cells compress intratumour vessels. Nature 2004;427:695. [PubMed: 14973470]
15. Roose T, Netti PA, Munn LL, Boucher Y, Jain RK. Solid stress generated by spheroid growth estimated using a linear poroelasticity model. Microvasc Res 2003;66:204–12. [PubMed: 14609526]
16. Leunig M, Yuan F, Menger MD, Boucher Y, Goetz AE, Messmer K, et al. Angiogenesis, microvascular architecture, microhemodynamics, and interstitial fluid pressure during early

growth of human adenocarcinoma LS174T in SCID mice. Cancer Res 1992;52:6553–60. [PubMed: 1384965]

17. Fukumura D, Salehi HA, Witwer B, Tuma RF, Melder RJ, Jain RK. Tumor necrosis factor α-induced leukocyte adhesion in normal and tumor vessels: effect of tumor type, transplantation site, and host strain. Cancer Res 1995;55:4824–9. [PubMed: 7585514]
18. Fukumura D, Yuan F, Endo M, Jain RK. Role of nitric oxide in tumor microcirculation: blood flow, vascular permeability, and leukocyte-endothelial interactions. Am J Pathol 1997;150:713–25. [PubMed: 9033284]
19. Fukumura D, Yuan F, Monsky WL, Chen Y, Jain RK. Effect of host microenvironment on the microcirculation of human colon adenocarcinoma. Am J Pathol 1997;151:679–88. [PubMed: 9284816]
20. Carmeliet P, Jain RK. Angiogenesis in cancer and other diseases: from genes to function to therapy. Nature 2000;407:249–57. [PubMed: 11001068]
21. Ohkubo C, Bigos D, Jain RK. Interleukin 2 induced leukocyte adhesion to the normal and tumor microvascular endothelium in vivo and its inhibition by dextran sulfate: implications for vascular leak syndrome. Cancer Res 1991;51:1561–3. [PubMed: 1997196]
22. Wu NZ, Klitzman B, Dodge R, Dewhirst MW. Diminished leukocyte-endothelium interaction in tumor microvessels. Cancer Res 1992;52:4265–8. [PubMed: 1638539]
23. Jain RK, Koenig GC, Dellian M, Fukumura D, Munn LL, Melder RJ. Leukocyte-endothelial adhesion and angiogenesis in tumors. Cancer Metastasis Rev 1996;15:195–204. [PubMed: 8842491]
24. Jain, RK.; Munn, LL.; Fukumura, D.; Melder, RJ. In vitro and in vivo quantification of adhesion between leukocytes and vascular endothelium. In: Morgan, JR.; Yarmush, ML., editors. Methods in Molecular Medicine, Vol 18: Tissue Engineering Methods and Protocols. Totowa: Humana Press Inc; 1998. p. 553-75.
25. Sasaki A, Melder RJ, Whiteside TL, Herberman RB, Jain RK. Preferential localization of human adherent lymphokine-activated killer cells in tumor microcirculation. J Natl Cancer Inst 1991;83:433–7. [PubMed: 1999850]
26. Melder RJ, Salehi HA, Jain RK. Interaction of activated natural killer cells with normal and tumor vessels in cranial windows in mice. Microvasc Res 1995;50:35–44. [PubMed: 7476578]
27. Melder RJ, Koenig GC, Witwer BP, Safabakhsh N, Munn LL, Jain RK. During angiogenesis, vascular endothelial growth factor and basic fibroblast growth factor regulate natural killer cell adhesion to tumor endothelium. Nat Med 1996;2:992–7. [PubMed: 8782456]
28. Kim I, Moon SO, Park SK, Chae SW, Koh GY. Angiopoietin-1 reduces VEGF-stimulated leukocyte adhesion to endothelial cells by reducing ICAM-1, VCAM-1, and E-selectin expression. Circ Res 2001;89:477–9. [PubMed: 11557733]
29. Zhang H, Issekutz AC. Growth factor regulation of neutrophil-endothelial cell interactions. J Leukoc Biol 2001;70:225–32. [PubMed: 11493614]
30. Detmar M, Brown LF, Schön MP, Elicker BM, Richard L, Velasco P, et al. Increased microvascular density and enhanced leukocyte rolling and adhesion in the skin of VEGF transgenic mice. J Invest Dermatol 1998;111:1–6. [PubMed: 9665379]
31. Jain RK, Safabakhsh N, Sckell A, Chen Y, Jiang P, Benjamin L, et al. Endothelial cell death, angiogenesis, and microvascular function after castration in an androgen-dependent tumor: role of vascular endothelial growth factor. Proc Natl Acad Sci USA 1998;95:10820–5. [PubMed: 9724788]
32. Tsuzuki Y, Fukumura D, Oosthuyse B, Koike C, Carmeliet P, Jain RK. Vascular endothelial growth factor (VEGF) modulation by targeting hypoxia-inducible factor-1alpha→hypoxia response element→VEGF cascade differentially regulates vascular response and growth rate in tumors. Cancer Res 2000;60:6248–52. [PubMed: 11103778]
33. Shojaei F, Wu X, Malik AK, Zhong C, Baldwin ME, Schanz S, et al. Tumor refractoriness to anti-VEGF treatment is mediated by CD11b+Gr1+ myeloid cells. Nat Biotech 2007;25:911–20.
34. Shojaei F, Wu X, Zhong C, Yu L, Liang XH, Yao J, et al. Bv8 regulates myeloid-cell-dependent tumour angiogenesis. Nature 2007;450:825–31. [PubMed: 18064003]

35. di Tomaso E, Capen D, Haskell A, Hart J, Logie JJ, Jain RK, et al. Mosaic tumor vessels: cellular basis and ultrastructure of focal regions lacking endothelial cell markers. Cancer Res 2005;65:5740–9. [PubMed: 15994949]
36. McDonald DM, Choyke PL. Imaging of angiogenesis: from microscope to clinic. Nat Med 2003;9:713–25. [PubMed: 12778170]
37. Chang YS, di Tomaso E, McDonald DM, Jones RC, Jain RK, Munn LL. Mosaic blood vessels in tumors: frequency of cancer cells in contact with flowing blood. Proc Natl Acad SCI USA 2000;97:14608–13. [PubMed: 11121063]
38. Dvorak, HF.; Nagy, JA.; Feng, D.; Dvorak, AM. Tumor architecture and targeted delivery. In: Abrams, PG.; Fritzberg, AR., editors. Radioimmunotherapy of Cancer. New York: Marcel Dekker, Inc; 2002. p. 107-35.
39. Winkler F, Kozin SV, Tong R, Chae S, Booth MF, Garkavtsev I, et al. Kinetics of vascular normalization by VEGFR2 blockade governs brain tumor response to radiation: role of oxygenation, angiopoietin-1 and matrix metalloproteinases. Cancer Cell 2004;6:553–63. [PubMed: 15607960]
40. Gerlowski LE, Jain RK. Microvascular permeability of normal and neoplastic tissues. Microvasc Res 1986;31:288–305. [PubMed: 2423854]
41. Yuan F, Leunig M, Berk DA, Jain RK. Microvascular permeability of albumin, vascular surface area, and vascular volume measured in human adenocarcinoma LS174T using dorsal chamber in SCID mice. Microvasc Res 1993;45:269–89. [PubMed: 8321142]
42. Hobbs SK, Monsky WL, Yuan F, Roberts G, Griffith L, Torchillin V, et al. Regulation of transport pathways in tumor vessels: role of tumor type and host microenvironment. Proc Natl Acad Sci USA 1998;95:4607–12. [PubMed: 9539785]
43. Jain RK. Transport of molecules across tumor vasculature. Cancer Metastasis Rev 1987;6:559–93. [PubMed: 3327633]
44. Monsky WL, Fukumura D, Gohongi T, Ancukiewcz M, Weich HA, Torchilin VP, et al. Augmentation of transvascular transport of macromolecules and nanoparticles in tumors using vascular endothelial growth factor. Cancer Res 1999;59:4129–35. [PubMed: 10463618]
45. Yuan F, Dellian M, Fukumura D, Leunig M, Berk DA, Torchilin VP, et al. Vascular permeability in a human tumor xenograft: molecular size dependence and cutoff size. Cancer Res 1995;55:3752–6. [PubMed: 7641188]
46. Kadambi A, Carreira CM, Yun C, Padera TP, Dolmans DEGJ, Carmeliet P, et al. Vascular endothelial growth factor (VEGF)-C differentially affects tumor vascular function and leukocyte recruitment: role of VEGF-receptor 2 and host VEGF-A. Cancer Res 2001;61:2404–8. [PubMed: 11289105]
47. Willett CG, Boucher Y, di Tomaso E, Duda DG, Chung DC, Sahani DV, et al. Direct evidence that the anti-VEGF antibody Bevacizumab has anti-vascular effects in human rectal cancer. Nat Med 2004;10:145–7. [PubMed: 14745444]
48. Batchelor TT, Sorensen AG, di Tomaso E, Zhang WT, Duda DG, Cohen KS, et al. AZD2171, a pan-VEGF receptor tyrosine kinase inhibitor, normalizes tumor vasculature and alleviates edema in blioblastoma patients. Cancer Cell 2007;11:83–95. [PubMed: 17222792]
49. Leu AJ, Berk DA, Yuan F, Jain RK. Flow velocity in the superficial lymphatic network of the mouse tail. Am J Physiol 1994;267:H1507–13. [PubMed: 7943396]
50. Berk DA, Swartz MA, Leu AJ, Jain RK. Transport in lymphatic capillaries. II. Microscopic velocity measurement with fluorescence photobleaching. Am J Physiol 1996;270:H330–7. [PubMed: 8769769]
51. Swartz MA, Berk DA, Jain RK. Transport in lymphatic capillaries. I. Macroscopic measurements using residence time distribution theory. Am J Physiol 1996;270:H324–9. [PubMed: 8769768]
52. Leu AJ, Berk DA, Lymboussaki A, Alitalo K, Jain RK. Absence of functional lymphatics within a murine sarcoma: a molecular and functional evaluation. Cancer Res 2000;60:4324–7. [PubMed: 10969769]
53. Padera TP, Kadambi A, di Tomaso E, Carreira CM, Brown EB, Boucher Y, et al. Lymphatic metastasis in the absence of functional intratumor lymphatics. Science 2002;296:1883–6. [PubMed: 11976409]

54. Jeltsch M, Kaipainen A, Joukov V, Meng X, Lasko M, Rauvala H, et al. Hyperplasia of lymphatic vessels in VEGF-C transgenic mice. Science 1997;276:1423–5. [PubMed: 9162011]
55. Jain RK, Tong R, Munn LL. Effect of vascular normalization by antiangiogenic therapy on interstitial hypertension, peritumor edema, and lymphatic metastasis: insights from a mathematical model. Cancer Res 2007;67:2729–35. [PubMed: 17363594]
56. Jain RK. Barriers to drug delivery in solid tumors. Sci Am 1994;271:58–65. [PubMed: 8066425]
57. Jain RK, Fenton BT. Intra-tumor lymphatic vessels: a case of mistaken identity or malfunction. J Natl Cancer Inst 2002;94:417–21. [PubMed: 11904313]
58. Hoshida T, Isaka N, Hagendoorn J, di Tomaso E, Chen YL, Pytowski B, et al. Imaging steps of lymphatic metastasis reveals that vascular endothelial growth factor-C increases metastasis by increasing delivery of cancer cells to lymph nodes: therapeutic implications. Cancer Res 2006;66:8065–75. [PubMed: 16912183]
59. Helmlinger G, Yuan F, Dellian M, Jain RK. Interstitial pH and pO_2 gradients in solid tumors in vivo: high-resolution measurements reveal a lack of correlation. Nat Med 1997;3:177–82. [PubMed: 9018236]
60. Harris AL. Hypoxia: a key regulatory factor in tumour growth. Nat Rev Cancer 2002;2:38–47. [PubMed: 11902584]
61. Tatum JL, Kelloff GJ, Gillies RJ, Arbeit JM, Brown JM, Chao KS, et al. Hypoxia: importance in tumor biology, noninvasive measurement by imaging, and value of its measurement in the management of cancer therapy. Int J Radiat Biol 2006;82:699–757. [PubMed: 17118889]
62. Brown JM, Giaccia AJ. The unique physiology of solid tumors: opportunities (and problems) for cancer therapy. Cancer Res 1998;58:1408–16. [PubMed: 9537241]
63. Dewhirst MW. Concepts of oxygen transport at the microcirculatory level. Semin Radiat Oncol 1998;8:143–50. [PubMed: 9634491]
64. Tredan O, Galmarini CM, Patel K, Tannock IF. Drug resistance and the solid tumor microenvironment. J Natl Cancer Inst 2007;99:1441–54. [PubMed: 17895480]
65. Brown JM. The hypoxic cell: a target for selective cancer therapy—Eighteenth Bruce F. Cain Memorial Award lecture. Cancer Res 1999;59:5863–70. [PubMed: 10606224]
66. Erler JT, Bennewith KL, Nicolau M, Dornhofer N, Kong C, Le QT, et al. Lysyl oxidase is essential for hypoxia-induced metastasis. Nature 2006;440:1222–6. [PubMed: 16642001]
67. Pennacchietti S, Michieli P, Galluzzo M, Mazzone M, Giordano S, Comoglio PM. Hypoxia promotes invasive growth by transcriptional activation of the met protooncogene. Cancer Cell 2003;3:347–61. [PubMed: 12726861]
68. Rofstad EK, Mathiesen B, Kindem K, Galappathi K. Acidic extracellular pH promotes experimental metastasis of human melanoma cells in athymic nude mice. Cancer Res 2006;66:6699–707. [PubMed: 16818644]
69. Fukumura, D. Role of microenvironment on gene expression, angiogenesis and microvascular functions in tumors. In: Meadows, GG., editor. Integration/Interaction of Oncologic Growth. Dordrecht: Springer Science+Business Media B.V; 2005. p. 23-36.
70. Fukumura D, Xavier R, Sugiura T, Chen Y, Park EC, Lu NF, et al. Tumor induction of VEGF promoter activity in stromal cells. Cell 1998;94:715–25. [PubMed: 9753319]
71. Fukumura D, Xu L, Chen Y, Gohongi T, Seed B, Jain RK. Hypoxia and acidosis independently up-regulate vascular endothelial growth factor transcription in brain tumors in vivo. Cancer Res 2001;61:6020–4. [PubMed: 11507045]
72. Semenza GL. Targeting HIF-1 for cancer therapy. Nat Rev Cancer 2003;3:721–32. [PubMed: 13130303]
73. Xu L, Pathak PS, Jain RK, Fukumura D. Hypoxia-induced activation of p38 mitogen-activated protein kinase and phosphatidylinositol 3′-kinase signaling pathways contributes to expression of interleukin-8 in human ovarian carcinoma cells. Clin Cancer Res 2004;10:701–7. [PubMed: 14760093]
74. Xu L, Fukumura D, Jain RK. Acidic extracellular pH induces vascular endothelial growth factor (VEGF) in human glioblastoma cells via ERK1/2 MAPK signaling pathway. Mechanism of low pH-induced VEGF. J Biol Chem 2002;277:11368–74. [PubMed: 11741977]

75. Martin GR, Jain RK. Fluorescence ratio imaging measurement of pH gradients: calibration and application in normal and tumor tissues. Microvasc Res 1993;46:216–30. [PubMed: 8246820]
76. Torres-Filho IP, Leunig M, Yuan F, Intaglietta M, Jain RK. Noninvasive measurement of microvascular and interstitial oxygen profiles in a human tumor in SCID mice. Proc Natl Acad USA 1994;91:2081–5.
77. Weinberg, RA. The Biology of Cancer. New York: Garland Science Publishing; 2006.
78. Elenbaas B, Weinberg RA. Heterotypic signaling between epithelial tumor cells and fibroblasts in carcinoma formation. Exp Cell Res 2001;264:169–84. [PubMed: 11237532]
79. Li G, Satyamoorthy K, Meier F, Berking C, Bogenrieder T, Herlyn M. Function and regulation of melanoma–stromal fibroblast interactions: when seeds meet soil. Oncogene 2003;22:3162–71. [PubMed: 12789292]
80. Pollard JW. Tumour-educated macrophages promote tumour progression and metastasis. Nat Rev Cancer 2004;4:71–8. [PubMed: 14708027]
81. Tlsty TD. Stromal cells can contribute oncogenic signals. Semin Cancer Biol 2001;11:97–104. [PubMed: 11322829]
82. Liotta LA, Kohn EC. The microenvironment of the tumour–host interface. Nature 2001;411:375–9. [PubMed: 11357145]
83. Ruiter DJ, van Krieken JH, van Muijen GN, de Waal RM. Tumour metastasis: is tissue an issue? Lancet Oncol 2001;2:109–12. [PubMed: 11905791]
84. Noel A, De Pauw-Gillet MC, Purnell G, Nusgens B, Lapiere CM, Foidart JM. Enhancement of tumorigenicity of human breast adenocarcinoma cells in nude mice by matrigel and fibroblasts. Br J Cancer 1993;68:909–15. [PubMed: 8217606]
85. Orimo A, Gupta PB, Sgroi DC, Arenzana-Seisdedos F, Delaunay T, Naeem R, et al. Stromal fibroblasts present in invasive human breast carcinomas promote tumor growth and angiogenesis through elevated SDF-1/CXCL12 secretion. Cell 2005;121:335–48. [PubMed: 15882617]
86. Karnoub AE, Dash AB, Vo AP, Sullivan A, Brooks MW, Bell GW, et al. Mesenchymal stem cells within tumour stroma promote breast cancer metastasis. Nature 2007;449:557–63. [PubMed: 17914389]
87. de Visser KE, Eichten A, Coussens LM. Paradoxical roles of the immune system during cancer development. Nat Rev Cancer 2006;6:24–37. [PubMed: 16397525]
88. Tsuzuki Y, Carreira CM, Bockhorn M, Xu L, Jain RK, Fukumura D. Pancreas microenvironment promotes VEGF expression and tumor growth: novel window models for pancreatic tumor angiogenesis and microcirculation. Lab Invest 2001;81:1439–52. [PubMed: 11598156]
89. Fidler IJ. Angiogenic heterogeneity: regulation of neoplastic angiogenesis by the organ microenvironment. J Natl Cancer Inst 2001;93:1040–1. [PubMed: 11459857]
90. Kashiwagi S, Izumi Y, Gohongi T, Demou ZN, Xu L, Huang PL, et al. NO mediates mural cell recruitment and vessel morphogenesis in murine melanomas and tissue-engineered blood vessels. J Clin Invest 2005;115:1816–27. [PubMed: 15951843]
91. Jain RK. The Eugene M. Landis Award Lecture. Delivery of molecular and cellular medicine to solid tumors. Microcirculation 1997;4:1–23. [PubMed: 9110280]
92. Singh RK, Bucana CD, Gutman M, Fan D, Wilsaon MR, Fidler IJ. Organ site-dependent expression of basic fibroblast growth factor in human renal cell carcinoma cells. Am J Pathol 1994;145:365–74. [PubMed: 8053494]
93. Gutman M, Singh RK, Xie K, Bucana CD, Fidler IJ. Regulation of interleukin-8 expression in human melanoma cells by the organ environment. Cancer Res 1995;55:2470–5. [PubMed: 7758001]
94. Gohongi T, Fukumura D, Boucher Y, Yun CO, Soff GA, Compton C, et al. Tumor-host interactions in the gallbladder suppress distal angiogenesis and tumor growth: involvement of transforming growth factor β1. Nat Med 1999;5:1203–8. [PubMed: 10502827]
95. Dellian M, Witwer BP, Salehi HA, Yuan F, Jain RK. Quantitation and physiological characterization of angiogenic vessels in mice: effect of basic fibroblast growth factor, vascular endothelial growth factor/vascular permeability factor, and host microenvironment. Am J Pathol 1996;149:59–72. [PubMed: 8686763]

96. Monsky WL, Carreira CM, Tsuzuki Y, Gohongi T, Fukumura D, Jain RK. Role of host microenvironment in angiogenesis and microvascular functions in human breast cancer xenografts: mammary fat pad vs. cranial tumors. Clin Cancer Res 2002;8:1008–13. [PubMed: 11948107]

97. Bouloumie A, Lolmede K, Sengenes C, Galitzky J, Lafontan M. Angiogenesis in adipose tissue. Ann Endocrinol (Paris) 2002;63:91–5. [PubMed: 11994668]

98. Miyazawa-Hoshimoto S, Takahashi K, Bujo H, Hashimoto N, Saito Y. Elevated serum vascular endothelial growth factor is associated with visceral fat accumulation in human obese subjects. Diabetologia 2003;46:1483–8. [PubMed: 14534780]

99. Rupnick MA, Panigrahy D, Zhang CY, Dallabrida SM, Lowell BB, Langer R, et al. Adipose tissue mass can be regulated through the vasculature. Proc Natl Acad Sci USA 2002;99:10730–5. [PubMed: 12149466]

100. Kolonin MG, Saha PK, Chan L, Pasqualini R, Arap W. Reversal of obesity by targeted ablation of adipose tissue. Nat Med 2004;10:625–32. [PubMed: 15133506]

101. Fukumura D, Ushiyama A, Duda DG, Xu L, Tam J, Krishna V, et al. Paracrine regulation of angiogenesis and adipocyte differentiation during in vivo adipogenesis. Circ Res 2003;93:e88–97. [PubMed: 14525808]

102. Lijnen HR, Christiaens V, Scroyen I, Voros G, Tjwa M, Carmeliet P, et al. Impaired adipose tissue development in mice with inactivation of placental growth factor function. Diabetes 2006;55:2698–704. [PubMed: 17003333]

103. Folkman J, Shing Y. Angiogenesis. J Biol Chem 1992;267:10931–4. [PubMed: 1375931]

104. Sato TN, Tozawa Y, Deutsch U, Wolburg-Buchholz K, Fujiwara Y, Gendron-Maguire M, et al. Distinct roles of the receptor tyrosine kinases Tie-1 and Tie-2 in blood vessel formation. Nature 1995;376:70–4. [PubMed: 7596437]

105. Risau W, Sariola H, Zerwes HG, Sasse J, Ekblom P, Kemler R, et al. Vasculogenesis and angiogenesis in embryonic-stem-cell-derived embryoid bodies. Development 1988;102:471–8. [PubMed: 2460305]

106. Asahara T, Murohara T, Sullivan A, Silver M, van der Zee R, Li T, et al. Isolation of putative progenitor endothelial cells for angiogenesis. Science 1997;275:964–7. [PubMed: 9020076]

107. Simper D, Stalboerger PG, Panetta CJ, Wang S, Caplice NM. Smooth muscle progenitor cells in human blood. Circulation 2002;106:1199–204. [PubMed: 12208793]

108. Pettersson A, Nagy JA, Brown LF, Sundberg C, Morgan E, Jungles S, et al. Heterogeneity of the angiogenic response induced in different normal adult tissues by vascular permeability factor/vascular endothelial growth factor. Lab Invest 2000;80:99–115. [PubMed: 10653008]

109. Gerhardt H, Golding M, Fruttiger M, Ruhrberg C, Lundkvist A, Abramsson A, et al. VEGF guides angiogenic sprouting utilizing endothelial tip cell filopodia. J Cell Biol 2003;161:1163–77. [PubMed: 12810700]

110. Hirschi KK, D'Amore PA. Pericytes in the microvasculature. Cardiovasc Res 1996;32:687–98. [PubMed: 8915187]

111. Hirschi KK, Skalak TC, Peirce SM, Little CD. Vascular assembly in natural and engineered tissues. Ann N Y Acad Sci 2002;961:223–42. [PubMed: 12081906]

112. Schechner JS, Nath AK, Zheng L, Kluger MS, Hughes CC, Sierra-Honigmann MR, et al. In vivo formation of complex microvessels lined by human endothelial cells in an immunodeficient mouse. Proc Natl Acad Sci USA 2000;97:9191–6. [PubMed: 10890921]

113. Koike N, Fukumura D, Gralla O, Au P, Schechner JS, Jain RK. Tissue engineering: creation of long-lasting blood vessels. Nature 2004;428:138–9. [PubMed: 15014486]

114. Wang ZZ, Au P, Chen T, Shao Y, Daheron LM, Bai H, et al. Endothelial cells derived from human embryonic stem cells form durable blood vessels in vivo. Nat Biotechnol 2007;25:317–8. [PubMed: 17322871]

115. Lu SJ, Feng Q, Caballero S, Chen Y, Moore MA, Grant MB, et al. Generation of functional hemangioblasts from human embryonic stem cells. Nat Methods 2007;4:501–9. [PubMed: 17486087]

116. Au P, Tam J, Fukumura D, Jain RK. Bone marrow derived mesenchymal stem cells facilitate engineering of long-lasting functional vasculature. Blood 2008;111:4551–8. [PubMed: 18256324]

117. Au P, Daheron LM, Duda DG, Cohen KS, Tyrrell JA, Lanning RM, et al. Differential in vivo potential of endothelial progenitor cells from human umbilical cord blood and adult peripheral blood to form functional long-lasting vessels. Blood 2008;111:1302–5. [PubMed: 17993613]
118. Melero-Martin JM, Khan ZA, Picard A, Wu X, Paruchuri S, Bischoff J. In vivo vasculogenic potential of human blood-derived endothelial progenitor cells. Blood 2007;109:4761–8. [PubMed: 17327403]
119. Izumi Y, Xu L, di Tomaso E, Fukumura D, Jain RK. Herceptin acts as an anti-angiogenic cocktail. Nature 2002;416:279–80. [PubMed: 11907566]
120. Tong RT, Boucher Y, Kozin SV, Winkler F, Hicklin DJ, Jain RK. Vascular normalization by vascular endothelial growth factor receptor 2 blockade induces a pressure gradient across the vasculature and improves drug penetration in tumors. Cancer Res 2004;64:3731–6. [PubMed: 15172975]
121. Lee CG, Heijn M, di Tomaso E, Griffon-Etienne G, Ancukiewicz M, Koike C, et al. Anti-vascular endothelial growth factor treatment augments tumor radiation response under normoxic or hypoxic conditions. Cancer Res 2000;60:5565–70. [PubMed: 11034104]
122. Huber PE, Bischof M, Jenne J, Heiland S, Peschke P, Saffrich R, et al. Trimodal cancer treatment: beneficial effects of combined antiangiogenesis, radiation, and chemotherapy. Cancer Res 2005;65:3643–55. [PubMed: 15867359]
123. Wildiers H, Guetens G, De Boeck G, Verbeken E, Landuyt B, Landuyt W, et al. Effect of anti-vascular endothelial growth factor treatment on the intratumoral uptake of CPT-11. Br J Cancer 2003;88:1979–86. [PubMed: 12799646]
124. Vosseler S, Mirancea N, Bohlen P, Mueller MM, Fusenig NE. Angiogenesis inhibition by vascular endothelial growth factor receptor-2 blockade reduces stromal matrix metalloproteinase expression, normalizes stromal tissue, and reverts epithelial tumor phenotype in surface heterotransplants. Cancer Res 2005;65:1294–305. [PubMed: 15735015]
125. Kozin SV, Boucher Y, Hicklin DJ, Bohlen P, Jain RK, Suit HD. Vascular endothelial growth factor receptor-2-blocking antibody potentiates radiation-induced long-term control of human tumor xenografts. Cancer Res 2001;61:39–44. [PubMed: 11196192]
126. Fukumura D, Kashiwagi S, Jain RK. Role of nitric oxide in tumour progression. Nat Rev Cancer 2006;6:521–34. [PubMed: 16794635]
127. Kashiwagi S, Tsukada K, Xu L, Miyazaki J, Kozin SV, Tyrrell JA, et al. Perivascular nitric oxide gradients normalize tumor vasculature. Nat Med 2008;14:255–7. [PubMed: 18278052]
128. Ferrara N, Alitaro K. Clinical application of angiogenic growth factors and their inhibitors. Nat Med 1999;5:1359–64. [PubMed: 10581076]
129. Kerbel RS. Tumor angiogenesis: past, present and the near future. Carcinogenesis 2000;21:505–15. [PubMed: 10688871]
130. Kleinfeld D, Mitra PP, Helmchen F, Denk W. Fluctuations and stimulus-induced changes in blood flow observed in individual capillaries in layers 2 through 4 of rat neocortex. Proc Natl Acad Sci USA 1998;95:15741–6. [PubMed: 9861040]
131. Lendvai B, Stern EA, Chen B, Svoboda K. Experience-dependent plasticity of dendritic spines in the developing rat barrel cortex in vivo. Nature 2000;404:876–81. [PubMed: 10786794]
132. Helmchen F, Denk W. New developments in multiphoton microscopy. Curr Opin Neurobiol 2002;12:593–601. [PubMed: 12367641]
133. Boppart S, Herrmann J, Pitris C, Stamper D, Brezinski M, Fujimoto J. High resolution optical coherence tomography-guided laser ablation of surgical tissue. J Surgical Res 1999;82:275–84.
134. Huang D, Swanson EA, Lin CP, Schuman JS, Stinson WG, Chang W, et al. Optical coherence tomography. Science 1991;254:1178–81. [PubMed: 1957169]
135. Fan GY, Fujisaki H, Miyawaki A, Tsay RK, Tsien RY, Ellisman MH. Video-rate scanning two-photon excitation fluorescence microscopy and ratio imaging with cameleons. Biophys J 1999;76:2412–20. [PubMed: 10233058]
136. Kim KH, Buehler C, So PTC. High-speed, two-photon scanning microscope. Appl Opt 1999;38:6004–9. [PubMed: 18324120]

137. Niesner R, Andresen V, Neumann J, Spiecker H, Gunzer M. The power of single and multibeam two-photon microscopy for high-resolution and high-speed deep tissue and intravital imaging. Biophys J 2007;93:2519–29. [PubMed: 17557785]

138. Padera TP, Stoll BR, So PTC, Jain RK. High-speed intravital multiphoton laser scanning microscopy of microvasculature, lymphatics, and leukocyte-endothelial interactions. Mol Imaging 2002;1:9–15. [PubMed: 12920856]

139. Delaney PM, Harris MR, King RG. Novel microscopy using fibre optic confocal imaging and its suitability for subsurface blood vessel imaging in vivo. Clin Exp Pharmacol Physiol 1993;20:197–8. [PubMed: 8467575]

140. Helmchen F, Fee MS, Tank DW, Denk W. A miniature head-mounted two-photon microscope. high-resolution brain imaging in freely moving animals. Neuron 2001;31:903–12. [PubMed: 11580892]

141. Dickensheets D, Kino G. Micromachined scanning confocal optical microscope. Opt Lett 1996;21:764–6. [PubMed: 19876151]

142. D'Hallewin MA, El Khatib S, Leroux A, Bezdetnaya L, Guillemin F. Endoscopic confocal fluorescence microscopy of normal and tumor bearing rat bladder. J Urol 2005;174:736–40. [PubMed: 16006967]

143. Jung JC, Mehta AD, Aksay E, Stepnoski R, Schnitzer MJ. In vivo mammalian brain imaging using one- and two-photon fluorescence microendoscopy. J Neurophysiol 2004;92:3121–33. [PubMed: 15128753]

144. Levene MJ, Dombeck DA, Kasischke KA, Molloy RP, Webb WW. In vivo multiphoton microscopy of deep brain tissue. J Neurophysiol 2004;91:1908–12. [PubMed: 14668300]

145. Weissleder R. A clearer vision for in vivo imaging. Nat Biotechnol 2001;19:316–7. [PubMed: 11283581]

146. Weissleder R, Ntziachristos V. Shedding light onto live molecular targets. Nat Med 2003;9:123–8. [PubMed: 12514725]

147. Stroh M, Zimmer JP, Duda DG, Levchenko TS, Cohen KS, Brown EB, et al. Quantum dots spectrally distinguish multiple species within the tumor milieu in vivo. Nat Med 2005;11:678–82. [PubMed: 15880117]

148. Berk DA, Yuan F, Leunig M, Jain RK. Direct in vivo measurement of targeted binding in a human tumor xenograft. Proc Natl Acad Sci USA 1997;94:1785–90. [PubMed: 9050856]

149. Yuan F, Leunig M, Huang SK, Berk DA, Papahadjopoulos D, Jain RK. Microvascular permeability and interstitial penetration of sterically stabilized (stealth) liposomes in a human tumor xenograft. Cancer Res 1994;54:3352–6. [PubMed: 8012948]

150. Martin GR, Jain RK. Noninvasive measurement of interstitial pH profiles in normal and neoplastic tissue using fluorescence ratio imaging microscopy. Cancer Res 1994;54:5670–4. [PubMed: 7923215]

151. Dewhirst M, Ong E, Braun R, Smith B, Klitzman B, Evans S, et al. Quantification of longitudinal tissue pO2 gradients in window chamber tumours: impact on tumor hypoxia. Br J Cancer 1999;79:1717–22. [PubMed: 10206282]

152. Zhang J, Ma Y, Taylor SS, Tsien RY. Genetically encoded reporters of protein kinase A activity reveal impact of substrate tethering. Proc Natl Acad Sci USA 2001;98:14997–5002. [PubMed: 11752448]

153. Ting AY, Kain KH, Klemke RL, Tsien RY. Genetically encoded fluorescent reporters of protein tyrosine kinase activities in living cells. Proc Natl Acad Sci USA 2001;98:15003–8. [PubMed: 11752449]

154. Roessel, Pv; Brand, AH. Imaging into the future: visualizing gene expression and protein interactions with fluorescent proteins. Nat Cell Biol 2002;4:E15–20. [PubMed: 11780139]

155. Huang P, McKee TD, Jain RK, Fukumura D. Green fluorescent protein (GFP)-expressing tumor model derived from a spontaneous osteosarcoma in a vascular endothelial growth factor (VEGF)-GFP transgenic mouse. Comp Med 2005;55:236–43. [PubMed: 16089171]

156. Duda DG, Fukumura D, Munn LL, Booth MF, Brown EB, Huang P, et al. Differential transplantability of tumor-associated stromal cells. Cancer Res 2004;64:5920–4. [PubMed: 15342367]

157. Chambers AF, MacDonald IC, Schmidt EE, Koop S, Morris VL, Khokha R, et al. Steps in tumor metastasis: new concepts from intravital videomicroscopy. Cancer Metastasis Rev 1995;14:279–301. [PubMed: 8821091]

158. Hoffman RM. Visualization of GFP-expressing tumors and metastasis in vivo. Biotechniques 2001;30:1016–26. [PubMed: 11355337]

159. Chishima T, Miyagi Y, Wang X, Yamaoka H, Shimada H, Moossa AR, et al. Cancer invasion and micrometastasis visulaized in live tissue by green fluorescenct protein expression. Cancer Res 1997;57:2042–7. [PubMed: 9158003]

160. Li C-Y, Shan S, Huang Q, Braun RD, Lanzen J, Hu K, et al. Initial stages of tumor cell-induced angiogenesis: evaluation via skin window chambers in rodent models. J Natl Cancer Inst 2000;92:143–7. [PubMed: 10639516]

161. Naumov GN, Wilson SM, MacDonald IC, Schmidt EE, Morris VL, Groom AC, et al. Cellular expression of green fluorescent protein, coupled with high-resolution in vivo videomicroscopy, to monitor steps in tumor metastasis. J Cell Sci 1999;112:1835–42. [PubMed: 10341203]

162. Wyckoff JB, Jones JG, Condeelis JS, Segall JE. A critical step in metastasis: in vivo analysis of intravasation at the primary tumor. Cancer Res 2000;60:2504–11. [PubMed: 10811132]

163. Naumov GN. Persistence of solitary mammary carcinoma cells in a secondary site: a possible contribution to dormancy. Cancer Res 2002;62:2162–8. [PubMed: 11929839]

164. Isaka N, Padera TP, Hagendoorn J, Fukumura D, Jain RK. Peritumor lymphatics induced by vascular endothelial growth factor-C exhibit abnormal function. Cancer Res 2004;64:4400–4. [PubMed: 15231646]

165. Ny A, Koch M, Schneider M, Neven E, Tong RT, Maity S, et al. A genetic Xenopus laevis tadpole model to study lymphangiogenesis. Nat Med 2005;11:998–1004. [PubMed: 16116431]

166. Brown E, McKee TD, di Tomaso E, Pluen A, Seed B, Boucher Y, et al. Dynamic imaging of collagen and its modulation in tumors in vivo using second harmonic generation. Nat Med 2003;9:796–801. [PubMed: 12754503]

167. Endrich B, Reinhold HS, Gross JF, Intaglietta M. Tissue perfusion inhomogeneity during early tumor growth in rats. J Natl Cancer Inst 1979;62:387–95. [PubMed: 283271]

168. Kimura H, Braun R, Ong E, Hsu R, Secomb T, Papahadjopoulos D, et al. Fluctuations in red cell flux in tumor microvessels can lead to transient hyoxia and reoxygenation in tumor parenchyma. Cancer Res 1996;56:5522–8. [PubMed: 8968110]

169. Endrich B, Intaglietta M, Reinhold HS, Gross JF. Hemodynamic characteristics in microcirculatory blood channels during early tumor growth. Cancer Res 1979;39:17–23. [PubMed: 761187]

170. Lichtenbeld HC, Yuan F, Michel CC, Jain RK. Perfusion of single tumor microvessels: application to vascular permeability measurement. Microcirculation 1996;3:349–57. [PubMed: 9086446]

171. Chary SR, Jain RK. Direct measurement of interstitial convection and diffusion of albumin in normal and neoplastic tissues by fluorescence photobleaching. Proc Natl Acad Sci USA 1989;86:5385–9. [PubMed: 2748592]

172. Alexandrakis G, Brown EB, Tong RT, McKee TD, Campbell RB, Boucher Y, et al. Two-photon fluorescence correlation microscopy reveals the two-phase nature of transport in tumors. Nat Med 2004;10:203–7. [PubMed: 14716306]

173. Fukumura D, Jain RK. Tumor microvasculature and microenvironment: targets for anti-angiogenesis and normalization. Microvasc Res 2007;74:72–84. [PubMed: 17560615]

174. Jain RK. Normalizing tumor vasculature with anti-angiogenic therapy: a new paradigm for combination therapy. Nat Med 2001;7:987–9. [PubMed: 11533692]

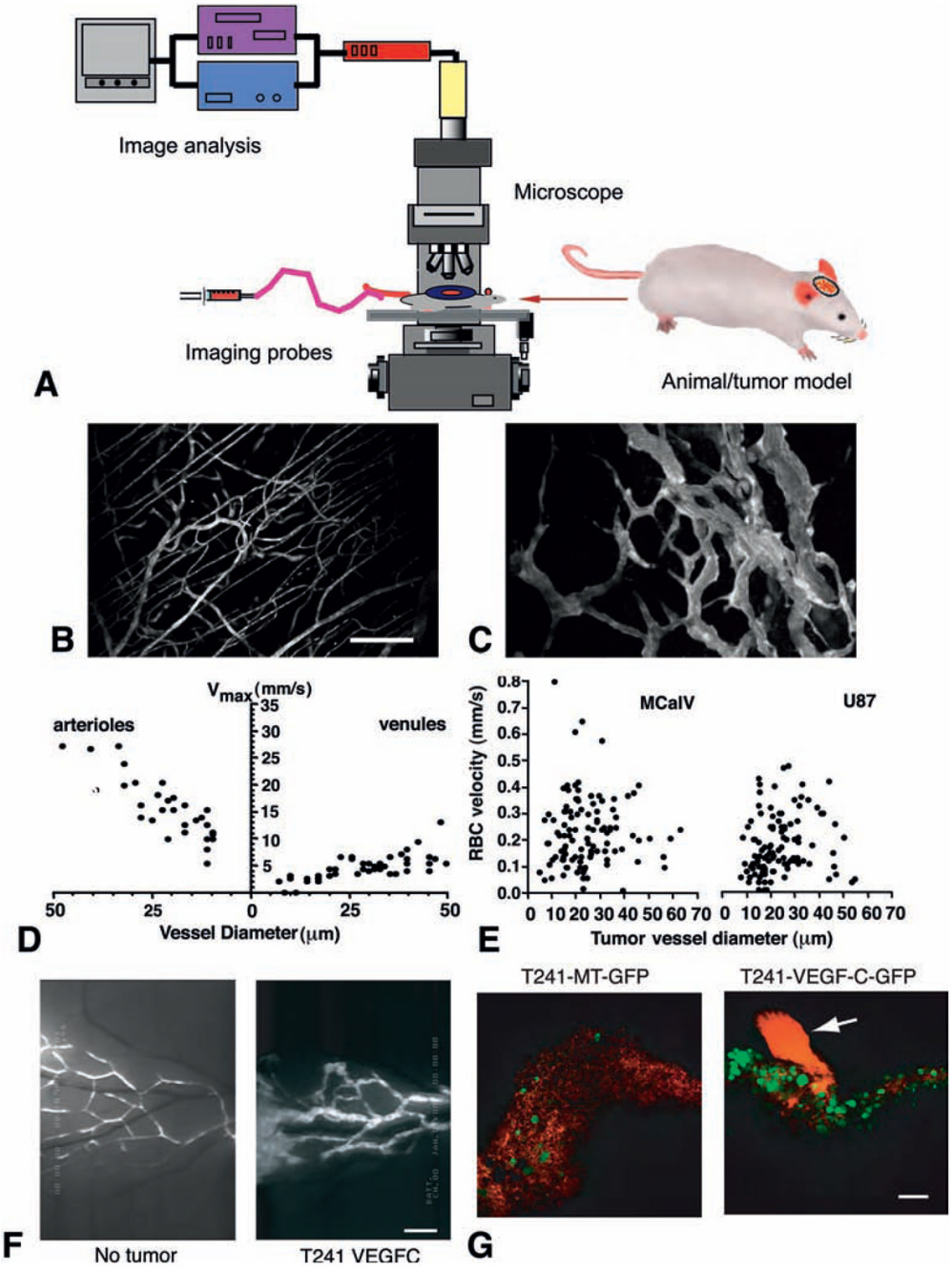

Fig. 1.

Imaging of tumor blood and lymphatic vessels. (A) Schematic intravital microscopy set up. An appropriate animal model, imaging probe(s), microscope, and image acquisition and analysis system are a prerequisite of intravital microscopy. (B–C) Multiphoton laser scanning microscopy image of normal blood vessels (B) and tumor vessels in LS174T human colon cancer xenografts (C) in mouse dorsal skin chambers. Blood vessels are contrast enhanced by FITC-dextran. Bar=100 μm. (D–E) Blood flow determined by intravital microscopy in normal pial vessels (maximum bead velocities, D) and tumor vessels in MCaIV murine breast cancer and U87 human glioma (RBC velocities, E) in mouse cranial windows. (F) FITC-dextran microlymphangiography of normal and peritumor

lymphatics in mouse ears. Bar=850 μm. Lymphatic vessels are hyperplastic in the peritumor region and ear base (further downstream) of the T241 fibrosarcomas overexpressing VEGF-C. (G) GFP-positive tumor cells (green) are observed entering the cervical lymph node from afferent lymphatic (red, arrow) by MPLSM. Bar=100 μm. VEGF-C overexpression significantly increases arrival of tumor cells in the lymph node. Macroscopic lymph node metastasis increases with the increase of tumor cell arrival in the lymph node (58). B–C, courtesy of Dr. Edward Brown; D–E, adapted from (7); F–G, adapted from (58).

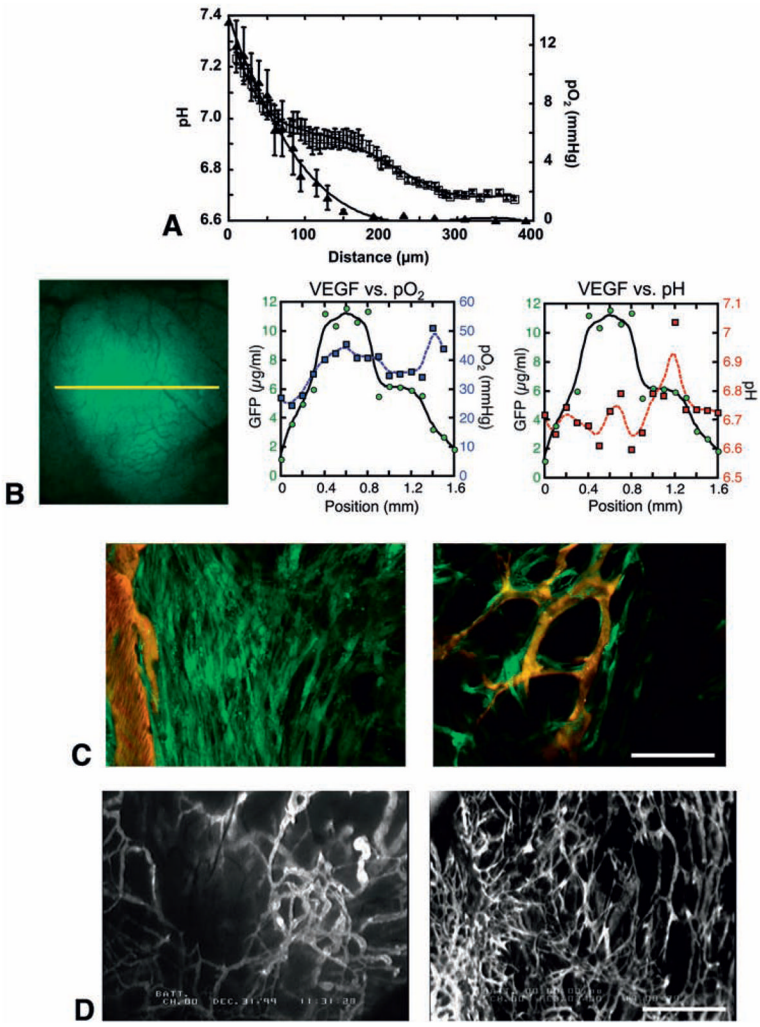

Fig. 2. Imaging of tumor microenvironment and role of host-tumor interaction in angiogenesis

(A) Mean interstitial pH and pO_2 profiles in LS174T tumors in the dorsal skin chambers as one moves away from the nearest blood vessels. Tissue pO_2 and pH were determined by phosphorescence quenching microscopy with a porphyrin probe and fluorescence ratio-imaging microscopy with BCECF, respectively. Open squares, pH; closed triangles, pO_2. X-axis corresponds to distance from the vessel wall. (B) VEGF promoter activity (green), tissue pO_2 (blue) and pH (red) in U87 tumors. *Left*, intravital microscopy image of GFP driven by VEGF promoter. The three parameters are determined along the yellow line. *Center*, this tumor is well oxygenated and there is no correlation between tissue pO_2 and VEGF promoter activity. *Right*, on the other hand, the peak of VEGF promoter activity is observed in the acidic pH region. (C) Imaging of VEGF promoter activity in host stromal cells. MCaIV murine breast tumor is grown in the dorsal skin chamber of a transgenic mouse expressing GFP under the control of VEGF promoter. *Left*, activated fibroblasts exhibit strong VEGF promoter activity (green) at the host-tumor interface. *Right*, VEGF expressing host cells associate with blood vessels (red) inside tumors. Bar=200 μm. (D) Microangiography of B16F10 murine melanoma grown in the dorsal skin chamber (*left*) and cranial window (*right*). Bar=1 mm. A, adapted from (59); B, adapted from (71); C, adapted from (4); D adapted from (173).

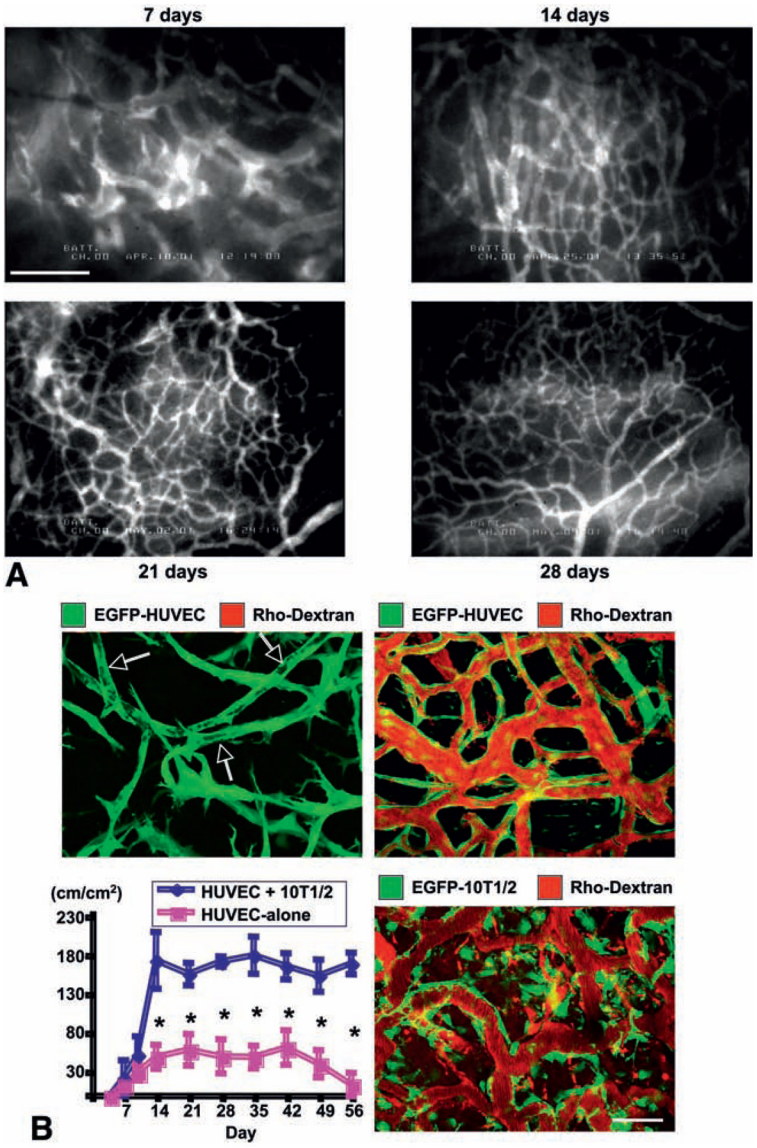

Fig. 3.

Imaging of physiological angiogenesis. (A) Angiogenesis and vessel remodeling during adipogenesis in the SCID mouse dorsal skinfold chamber after 3T3-F442A preadipocytes implantation. Blood vessels are contrast enhanced by the intravenous injection of FITC-dextran (2000 kDa). Bar=100 μm. (B) Morphological and functional analyses of engineered blood vessels. Vascular endothelial cells (HUVECs) and perivascular cell precursor cells (10T1/2 cells) or HUVECs alone were seeded in the collagen-fibronectin 3-D constructs and implanted in the cranial window in SCID mice. *Top*, 2-D projection of 3-D intravital multi-photon laser-scanning microscopy images of tissue-engineered blood vessels (EGFP expressing HUVEC, green; functional blood vessels contrast enhanced with rhodextran, red). *Top left*, 4 days after implantation of HUVEC+10T1/2 construct. Large vacuoles in the tubes resemble the lumens of capillaries (arrows) but they are not perfused (no red). *Top right*, 4 months after implantation of HUVEC+10T1/2 construct. Engineered vessels are stable and functional. *Bottom left*, Temporal changes in functional density of tissue-engineered blood vessels (total length of perfused vessel structure per unit area). N=4, mean

± SEM; *P<0.05. *Bottom right*, MPLSM image of engineered vessels, 4 weeks after implantation of HUVEC+EGFP-expressing 10T1/2 construct. Scale bar=50 μm. A, adapted from (101); B, adapted from (113).

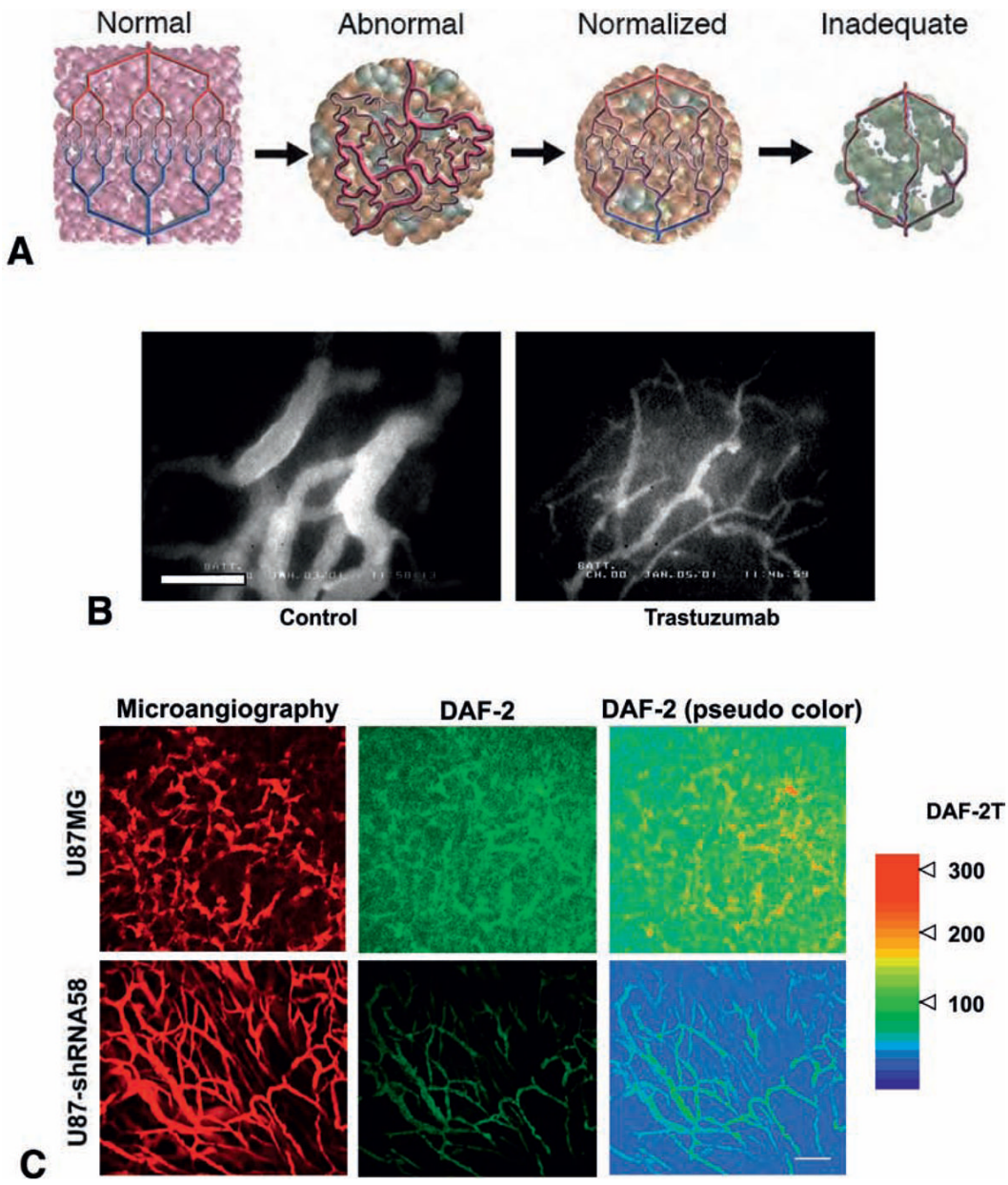

Fig. 4.

Tumor vascular normalization. (A) Changes in tumor vasculature during the course of anti-angiogenic therapy. Compared to the well-organized structure of normal vessels (Normal, *far left*), tumor vasculature is structurally and functionally abnormal (Abnormal, *middle left*). Anti-angiogenic therapies initially alleviate these abnormalities (Normalized, *middle right*). However, sustained or excessive anti-angiogenic treatments result in significant vessel reduction, and thus inadequate delivery of drugs or oxygen (Inadequate, *far right*). (B) Normalization of tumor vasculature by trastuzumab treatment. Microangiography in control and trastuzumab-treated MDA-MB-361HK tumors grown in the cranial window in SCID mice. Bar=100 μm. (C) Normalization of tumor vasculature by perivascular NO gradients. Tissue distribution of NO in U87 tumors grown in the cranial window in *Rag-1*$^{-/-}$ mice was visualized by means of DAF-2T fluorescence imaging using MPLSM. NO-sensitive fluorescence probe DAF-2 is converted to DAF-2T in the presence of NO,

increasing fluorescence by a factor of 200. Parental U87MG (*Top row*) or *nNOS*-shRNA58-transfected-U87 (*Bottom row*) tumors were studied. (*Left*) Microangiography using tetramethylrhodamine-dextran (2000 kDa). (*Middle*) Representative DAF-2T microfluorography captured 60 min after the loading of DAF-2 in tumors. (*Right*) Pseudocolor representation of DAF-2T microfluorographs. Color bar right shows calibration of the fluorescence intensity with known concentrations of DAF-2T. Bar=100 μm. A, adapted from (174); B, adapted from (119); C, adapted from (127).

TABLE 1

Examples of parameters measured and probes used in intravital microscopy

Parameter	Molecular probe	Reference
Molecular imaging		
Micropharmacokinetics	FITC-antibody, TMR-liposome	(148,149)
Microenvironment (pH, pO_2, NO)	BCECF, BSA-porphyrin, DAF-2	(59,76,90,127,150,151)
Enzyme activity (cathepsin B, protein kinase A, tyrosine kinase)	NIRF probe-graft copolymer, CFP-14–3-3τ-YFP reporter gene	(3,152,153)
Gene expression	GFP reporter gene	(4,70,71,154–156)
Cellular imaging		
Tracking cancer cells	GFP, calcein, fluorescent nanosphere	(37,58,157–163)
Tracking leukocytes	Rhodamine 6G, calcein	(4,17,21–23)
Tracking other cells	GFP, nanocrystals	(4,101,113,127,147)
Anatomical imaging		
Tumor size	Endogenous contrast, GFP, OCT	(16,158)
Vascular architecture (diameter, length, surface area, volume, branching patterns)	Endogenous contrast, OPS, fluorescent dextran, nanocrystals	(5,8,16,147,149)
Lymphatic architecture (diameter, length, branching patterns, valves)	Fluorescent dextran, nanocrystals	(49,50,53,58,138,164,165)
Extracellular matrix	Second harmonic generation (type I collagen)	(166)
Pore size	TMR-liposome/microsphere with varying size	(42,44)
Functional imaging		
Blood flow rate	Fluorescent dextran, RBC (fluorescent, endogenous contrast), OCT	(4,16,167–169)
Lymph flow rate	FITC dextran	(50,51,58)
Vascular permeability	TMR/Cy5-BSA, nanoparticles, nanocrystals	(4,40,41,147,170)
Interstitial diffusion, convection, and binding	Fluorescent BSA, IgG, dextran, liposome, nanoparticles	(148,171,172)

FITC, fluorescein isothiocyanate; TMR, tetremethylrhodamine; BCECF, 2′,7′-bis-(2-carboxyethyl)-5,6-carboxyfluorescein; BSA, bovine serum albumin; porphyrin, palladium meso-tetra (4-carboxyphenyl) porphyrin; NIRF, near-infrared fluorescence; CFP, cyan fluorescent protein; 14-3-3τ, phosphoamino acid binding domain; YFP, yellow fluorescent protein; GFP, green fluorescent protein; VEGFp, vascular endothelial growth factor promoter; OPS, orthogonal polarization spectral. This table is adapted and updated from (2).